High performance plasmonic crystal sensor formed by soft nanoimprint lithography

Viktor Malyarchuk, Feng Hua, Nathan H. Mack, Vanessa T. Velasquez, Jeffrey O. White, Ralph G. Nuzzo and John A. Rogers

Department of Materials Science and Engineering, University of Illinois at Urbana-Champaign, Urbana, IL 61801

jrogers@uiuc.edu

Abstract: This paper describes a new type of plasmonic sensor fabricated by imprint lithography using a soft, elastomeric mold. Angle-dependent, zero-order transmission experiments demonstrate the sensing potential of this device, which uses a two dimensional plasmonic crystal. Full angle-dependent mapping shows that the sensitivity to surface chemical binding events reaches maxima near regions of the plasmonic Brillouin zone where the dispersion curves of multiple surface plasmon polariton modes converge. This behavior, together with the simple, low cost procedures for building the structures, suggests a potentially important role for these devices in high performance chemical and biological sensing.

© 2005 Optical Society of America

OCIS codes: (000.2190) Experimental physics; (230.4000) Microstructure fabrication; (240.6680) Surface plasmons.

References and links

1. D. Diamond, ed., *Principles of chemical and biological sensors*, vol. 150 of *Chemical analysis* (Wiley, New York, 1998). "A Wiley-Interscience publication.".
2. J. Homola, S. S. Yee, and G. Gauglitz, "Surface plasmon resonance sensors: review," Sensors and Actuators B **54**, 3–15 (1999).
3. H. Raether, *Surface Plasmons on Smooth and Rough Surfaces and on Gratings* (Springer-Verlag, 1988).
4. A. G. Brolo, R. Gordon, B. Leathem, and K. L. Kavanagh, "Surface Plasmon Sensor Based on the Enhanced Light Transmission through Arrays of Nanoholes in Gold Films," Langmuir **20**(12), 4813–4815 (2004).
5. S. Chou, "Nanoimprint lithography and lithographically induced self-assembly," MRS Bulletin **26**(7), 512–518 (2001).
6. J. A. Rogers, "Rubber Stamping for Plastic Electronics and Fiber Optics," MRS Bulletin **26**(7), 530–534 (2001).
7. D. J. Resnick, S. V. Sreenivasan, and C. G. Willson, "Step & flash imprint lithography," Materials Today **8**(2), 34–42 (2005).
8. B. D. Gates, "Nanofabrication with molds & stamps," Materials Today **8**(2), 44–49 (2005).
9. J. A. Rogers and R. G. Nuzzo, "Recent progress in soft lithography," Materials Today **8**(2), 50–56 (2005).
10. S. Y. Chou, P. R. Krauss, and P. J. Renstrom, "Imprint lithography with 25-nanometer resolution," Science **272**, 85–87 (1996).
11. Y.-L. Loo, R. L. Willett, K. W. Baldwin, and J. A. Rogers, "Additive, nanoscale patterning of metal films with a stamp and a surface chemistry mediated transfer process: Applications in plastic electronics," Appl. Phys. Lett. **81**(3), 562–564 (2002).
12. Y.-L. Loo, R. L. Willett, K. W. Baldwin, and J. A. Rogers, "Interfacial chemistries for nanoscale transfer printing," J. Am. Chem. Soc. **124**(26), 7654–7655 (2002).
13. C. D. Bain, E. B. Troughton, Y.-T. Tao, J. Evall, G. M. Whitesides, and R. G. Nuzzo, "Formation of monolayer films by the spontaneous assembly of organic thiols from solution onto gold," J. Am. Chem. Soc. **111**(1), 321–335 (1989).

#7370 - $15.00 US
Received 5 May 2005; revised 8 July 2005; accepted 10 July 2005
(C) 2005 OSA

14. W. Ebbesen, H. J. Lezec, H. F. Ghaemi, T. Thio, and P. A. Wolff, "Extraordinary optical transmission through sub-wavelength hole arrays," Nature **391**(6668), 667–669 (1998).
15. E. Altewischer, M. P. van Exter, and J. P. Woerdman, "Plasmon-assisted transmission of entangled photons," Nature **418**, 304–306 (2002).
16. S. C. Hohng, Y. C. Yoon, D. S. Kim, V. Malyarchuk, R. Müller, C. Lienau, J. W. Park, K. H. Yoo, J. Kim, H. Y. Ryu, and Q. H. Park, "Light emission from the shadows: Surface plasmon nano-optics at near and far fields," Appl. Phys. Lett. **81**(17), 3239–3241 (2002).
17. D. S. Kim, S. C. Hohng, V. Malyarchuk, Y. C. Yoon, Y. H. Ahn, K. J. Yee, J. Park, J. Kim, Q. H. Park, and C. Lienau, "Microscopic Origin of Surface-Plasmon Radiation in Plasmonic Band-Gap Nanostructures," Phys. Rev. Lett. **91**(14), 143,901 (2003).
18. E. Devauxa and T. W. Ebbesen, "Launching and decoupling surface plasmons via micro-gratings," Appl. Phys. Lett. **83**(24), 4936–4938 (2003).
19. W. L. Barnes, W. A. Murray, J. Dintinger, E. Devaux, and T. Ebbesen, "Surface plasmon polaritons and their role in the enhanced transmission of light through periodic arrays of subwavelength holes in a metal film," Phys. Rev. Lett. **92**(10), 107,401 (2004).
20. F. Hua, Y. Sun, A. Gaur, M. A. Meitl, L. Bilhaut, L. Rotkina, J. Wang, P. Geil, M. Shim, J. A. Rogers, and A. Shim, "Polymer imprint lithography with molecular-scale resolution," Nano Lett. **4**(12), 2467–2471 (2004).
21. H. F. Ghaemi, T. Thio, D. E. Grupp, T. W. Ebbesen, and H. J. Lezec, "Surface plasmons enhance optical transmission through subwavelength holes," Phys. Rev. B **58**(11), 6779–6782 (1998).
22. P. B. Johnson and R. W. Christy, "Optical constants of the noble metals," Phys. Rev. B **6**(12), 4370–4379 (1972).
23. C. Ropers, D. J. Park, G. Stibenz, G. Steinmeyer, J. Kim, D. S. Kim, and C. Lienau, "Femtosecond Light Transmission and Subradiant Damping in Plasmonic Crystals," Phys. Rev. Lett. **94**(11), 113,901 (2005).

1. Introduction

The field of biosensing exploits many technologies that are optically based [1]. While heavily dominated by spectroscopic protocols that employ fluorescence, label-less methods that exploit the surface plasmon polariton (SPP) resonances of uniform metal films such as gold or silver have become increasingly important [2]. In such systems, the spectral position and the quality of resonance are completely defined by the intrinsic properties of the metal used, the thickness and refractive index of the analyte film, and the prism used to couple light into and out of the SPP [3]. These device features make it impossible to improve their performance by, for example, moving the SPP resonance to an absorption band of a molecule to be detected. (Some limited change in resonance position can be induced by changing the material, and therefore the index, of the coupling prism). One strategy for eliminating this restriction is to replace the prism-flat metal film combination with a metal grating. In this case, the geometry of the grating can be used to control the position of the SPP resonance and further provide capacities needed to develop new types of compact form factor sensors [4]. The required sub-micron features needed to couple SPPs with light at visible wavelengths are difficult, and expensive, to fabricate using conventional means. Low cost lithographic procedures based on printing and molding [5, 6, 7, 8, 9, 10, 11, 12] have the capabilities to fabricate high quality metal structures with the necessary dimensions needed to couple to the SPPs. This paper describes the use of a nanoimprinting technique that uses soft elastomeric molds and photo-curable polymers to form high resolution two dimensional plasmonic crystal sensors. Angle-dependent, zero-order transmission experiments using a model system consisting of an alkanethiolate self-assembled monolayer (SAM) on Au [13], reveal sensitivity "maps" for these devices. The results indicate high performance at angles that correspond to locations in the plasmonic Brillouin zone (PBZ) where dispersion curves of multiple SPPs converge.

2. Nanoprinted plasmonic crystal

Since the discovery of extraordinary optical transmission through subwavelength hole arrays [14], plasmonic crystals have attracted significant interest in the scientific community [15, 16, 17, 18, 19]. The required structures are typically fabricated either by electron beam

#7370 - $15.00 US Received 5 May 2005; revised 8 July 2005; accepted 10 July 2005
(C) 2005 OSA

lithography in a serial fashion over limited areas with imperfect spatial coherence, or by expensive, advanced forms of projection mode photolithography. A simple, soft imprinting procedure illustrated in Figure 1 formed the structures used for the work described here. Casting and cur-

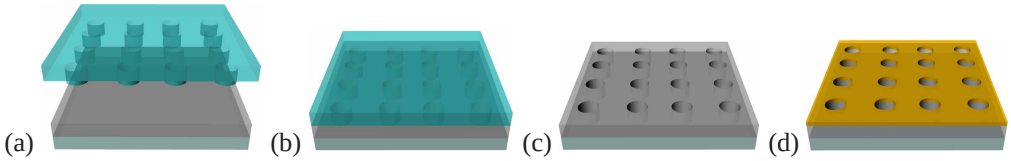

Fig. 1. Plasmonic crystal fabrication process: (a) imprinting; (b) curing; (c) removing; and (d) gold deposition.

ing a prepolymer of poly(dimethylsiloxane) (PDMS) against a master of photoresist on a silicon wafer, patterned by projection mode deep ultraviolet lithography, formed the molds according to the following procedures. The master was first placed in a vacuum chamber along with 100mL of (tridecafluoro-1,1,2,2-tetrahydrooctyl)-1-trichlorosilane (United Chemical Tech) for 2 hours. The resulting silane layer prevents adhesion of the PDMS to the bare SiO_2. The stamp was prepared as a bilayer of hard PDMS (h-PDMS) to reproduce accurately the master's features, and soft PDMS (s-PDMS) to provide a flexible support for the brittle h-PDMS. The h-PDMS (Gelest, Inc) was prepared as follows: 3.4g of poly(7-8% vinylmethylsiloxane)-(dimethylsiloxane), 100mg of (1,3,5,7-tetravinyl-1,3,5,7-tetramethylcyclotetrasiloxane) and 50mg of platinum catalyst were mixed and placed in a vacuum chamber for 5 minutes. After removal from the chamber, 1g poly(25-30% methylhydrosiloxane)-(dimethylsiloxane) was then added, mixed and the resulting sample was placed back into vacuum for 5 minutes. This prepolymer mixture was spin cast onto the master at 1000rpm for 300s and then baked at 65°C for 2 minutes. The s-PDMS (Sylgard 184, Dow Corning), prepared by mixing base and curing agent at a ratio of 10:1, was then poured onto the h-PDMS. The typical thicknesses used to construct the stamp were 10μm for the h-PDMS and 3mm for the s-PDMS. Baking at 65°C for 2 hours completed the curing of the polymers. Peeling the composite h-PDMS/s-PDMS replica away from the master completed the fabrication of a PDMS mold with the corresponding relief of the master. Many such molds can be produced from a single master, and each mold can be used many times. In the first step of the imprinting procedure, a layer of a photocurable polyurethane (PU) (NOA 73, Norland Products) was spin cast onto a glass slide (Fig. 1 (a)). Placing the PDMS mold into contact with this layer and then exposing it to ultraviolet light (350-380nm; long wavelength ultraviolet lamp, UVP) at $\sim$19mW/cm^2 for 1 hour through the transparent mold cured the polyurethane into a solid form (Fig. 1 (b)). The resulting PU film was $\sim 10\mu$m thick and presented a relief structure in the geometry of the PDMS stamp. Removing the mold (Fig. 1 (c)), completed the process. The imprinted polyurethane/glass substrate served as a dielectric template for the production of a plasmonic crystal by blanket evaporation of a thin layer of gold (50nm) on top of a titanium adhesion layer (5nm). The gold layer was selected to be sufficiently thin to enable operation in transmission mode but thick enough to support SPPs. These simple, low cost fabrication procedures are reliable, robust, and can be applied over large areas. The resolution is exceptionally high; relief features as small as 1-2nm have been successfully produced with this method [20].

Figure 2 shows scanning electron micrographs of a typical device. The crystal used in this work has a square lattice consisting of depressions with diameters and depths of 545nm and 300nm, respectively, and with a periodicity of 700nm. The walls of the depressions are not coated with metal, due to the directional nature of the gold flux in the electron beam evaporation system that was used.

#7370 - $15.00 US
Received 5 May 2005; revised 8 July 2005; accepted 10 July 2005
(C) 2005 OSA

(a) 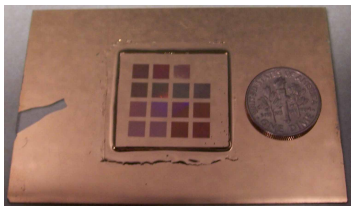 (b) 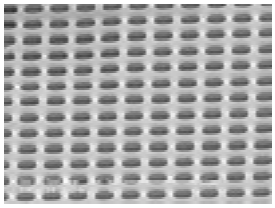 (c) 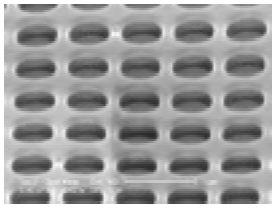

Fig. 2. Two dimensional plasmonic crystal sensor: (a) low resolution image; (b) scanning electron micrograph (SEM); (c) high resolution SEM showing that walls of the depression are free from metal.

The SPPs involve evanescent electromagnetic fields in the direction perpendicular to metal/dielectric interface. The depth of the depressions (300nm) is comparable to the SPP penetration depth into the dielectric medium. In such a geometry, our system consists of a plasmonic crystal (continuous metallic layer on the upper surface) weakly coupled to an array of isolated metallic islands (bottom of the depressions).

3. Experiment and results

We performed zero-order transmission experiments in order to obtain the PBZ map of these structures [21, 16, 19]. The scheme of the setup is presented in Fig. 3. The sample was fixed

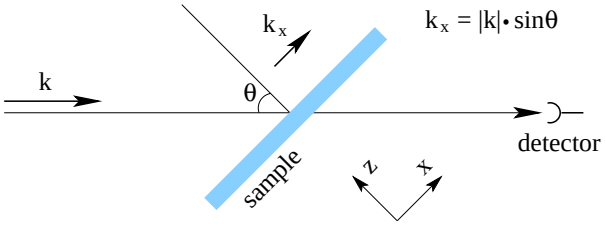

Fig. 3. Experimental zero-order transmission setup.

on a 2-axis rotation stage mounted inside of a UV-Vis-NIR spectrophotometer (Cary 5G). One axis turned the device to the required polar angle of incidence θ. The other rotated the sample around the Z axis (Fig. 3). This stage defines the direction for excitation and propagation of the plasmonic modes on the metal surface. The transmission spectra have a nominal spectral resolution of 1nm, and are collected in a dual beam configuration to account for any intensity fluctuations in the light source.

PBZ maps were acquired by fixing the desired polar angle of incidence (θ) and recording a transmission spectrum over a predefined wavelength range. The angle θ was varied between 0° and 75° with incremented steps of 0.5°. Two main directions inside PBZ were mapped. One corresponded to the Γ – X direction (sample rotated along the axis perpendicular to the grating period), the other to the Γ – M direction (sample rotated around the axis perpendicular to the grating diagonal).

The baseline for background correction was measured using the unstructured and uncoated region of the sample. The 50nm thick gold film was slightly transparent at a level consistent with expectations for an unstructured film. In contrast, the plasmonic crystal shows strong resonances in transmission intensity [14] that reach ∼14% at the maximum and ∼0.3% at the minimum for our sample at normal incidence. The overall tramsmission intensity decreases as

#7370 - $15.00 US
Received 5 May 2005; revised 8 July 2005; accepted 10 July 2005
(C) 2005 OSA

the polar angle (θ) increases and shows a value of $\sim$5% at the maximum and $\sim$0.3% at the minimum for $\theta = 75^{\circ}$. This spectra are then used for PBZ mapping. The momentum of the SPP at the Γ-point in the PBZ is $k_{spp_\Gamma} = 0$, at X, $k_{spp_X} = \pi/p$, and at M, $k_{spp_M} = \pi/(d/2)$, where p is the period of the grating and d its diagonal.

The PBZ of the plasmonic crystal measured immediately after gold deposition is presented in Fig. 4 (a). The surface sensing capability of the device was tested by measuring a sample

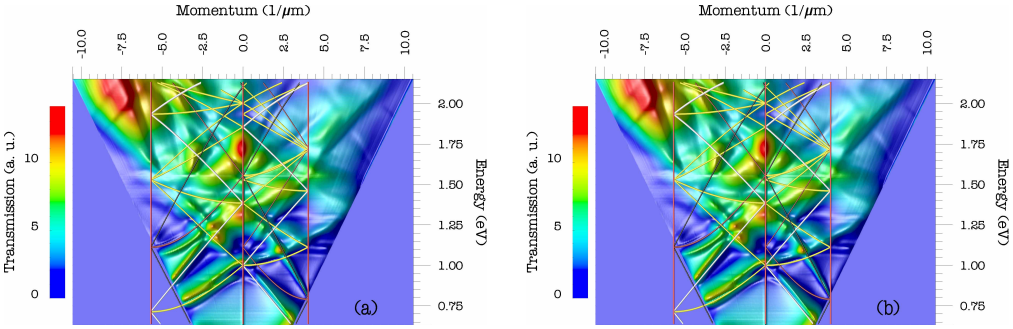

Fig. 4. Plasmonic Brillouin zones (a) before and (b) after the formation of a hexadecanethiol SAM.

with a self assembled monolayer (SAM) on the exposed gold formed by contact transfer from 1mM ethanolic solution of hexadecanethiol [13]. Slight changes in the plasmonic dispersion caused by the formation of the SAM are evident upon visual inspection, as revealed by the data presented in Fig. 4 (b). The large blue triangular regions in the lower left and right corners of Fig. 4 correspond to regions that lie beyond the rotation stage's upper limit of $\theta = 75^{\circ}$.

In order to highlight the effects of the SAM on the PBZ, we recast the data in the form of a sensitivity map using equation (1).

$$Sensitivity = Transmission_{SAM} - Transmission_{initial} \tag{1}$$

The resulting image is presented in Fig. 5 (a). The essence of any sensing application is in the

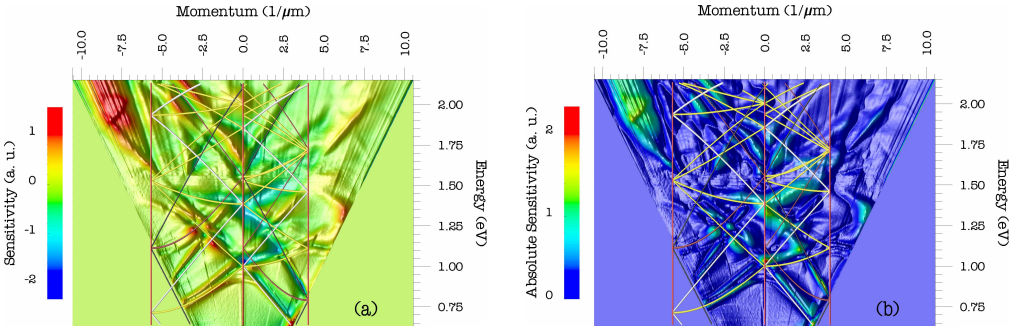

Fig. 5. Plasmonic crystal surface sensitivity: (a) sensitivity map; (b) absolute values of the sensitivity map.

accurate detection of the change in signal (here a shift in the position and intensity of the SPP resonances) due to the presence of an analyte. A straightforward way to visualize the response

#7370 - $15.00 US
Received 5 May 2005; revised 8 July 2005; accepted 10 July 2005
(C) 2005 OSA

is to examine only the absolute values of such changes. The corresponding absolute sensitivity map is shown in Fig. 5 (b).

The simplest approach to describe the plasmonic Brillouin zone is to utilize the dispersion relation for SPPs on a smooth metal surface (2) [3].

$$k_{spp} = \frac{\omega}{c}\sqrt{\frac{\varepsilon_d \cdot \varepsilon_m}{\varepsilon_d + \varepsilon_m}} \tag{2}$$

Here ω is the SPP frequency, c is the speed of light, ε_d and ε_m are the respective dielectric constants for the corresponding dielectric and the metallic media. The value ε_m is complex and strongly dependent on frequency. We obtained the dispersion relation of the SPP using experimental data for the dielectric constant of gold [22]. One can build the PBZ by taking into account the periodicity of the plasmonic crystal and folding the SPP dispersion line at the corresponding critical points. The results of this analysis are superimposed onto Figs. 4 and 5. The black and brown lines represent SPPs localized at the metal/air interface of the plasmonic crystal and propagating in directions perpendicular and parallel to the rotation axis, respectively. The white and yellow lines represent SPPs lying at the metal/polyurethane interface and propagating in directions perpendicular and parallel to the rotation axis, respectively. The red lines represent the critical points: the left line is the M-point; the middle line is the Γ-point; and the right line is the X-point. The use of the folded dispersion relation for a flat metal is an oversimplification of this grating system. While delivering fairly good agreement for most of the SPP resonance bands, this model is not able to correctly describe all of the features observed in the PBZ. A complete description is the subject of current work.

The sensitivity map shows that regions with strong resonances exhibit high sensitivity. Some increased sensitivity regions occur, however, near intersections of SPPs on the substrate/metal and air/metal interfaces. At these locations, coupling between the modes can be expected, leading an increase in lifetime and propagation length of the SPP [23]. The highest sensitivity occurs at Γ-point (maximum ∼1.03eV) where 5 substrate/metal and 1 air/metal mode are interacting.

The trends in sensitivity can be better understood from spectra extracted from the maps. The data shown in Figure 6 correspond to representative angle-dependent transmission spectra

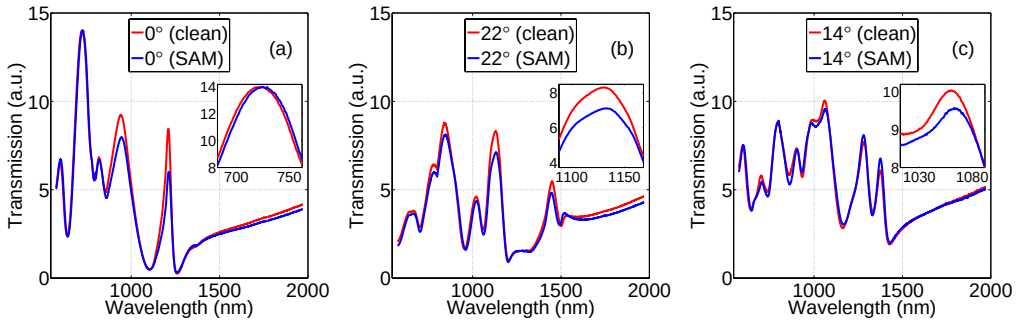

Fig. 6. Transmission spectra at chosen points: (a) 0° (Γ-point); (b) 22° in Γ–X region (maximum sensitivity at $k_x = 2.1\mu m$); and (c) 14° in Γ–M region (maximum sensitivity at $k_x = -1.2\mu m$). Insets show the magnified parts of the spectra in order to highlight the change due to the formation of a hexadecanethiol SAM.

measured for both a clean and a SAM-modified sensor. Spectra are shown for the Γ-point and for regions where air/metal and substrate/metal modes are overcrossing and device show anomalously high sensitivity. Fig. 6 (b) is for the Γ–X region and Fig. 6 is for Γ–X region. The wavelength shifts of the resonances in Fig. 6 correlate well with the types of responses seen

#7370 - $15.00 US
Received 5 May 2005; revised 8 July 2005; accepted 10 July 2005
(C) 2005 OSA

in conventional SPR systems; these changes largely reflect a modest ($\sim$4nm) red shifting of the position of the resonance due to the refractive index change at the dielectric/metal interface that results from the formation of the $\sim$21Å thick SAM [13] on the surface. The changes of the relative intensities of the different resonances, however, are are more unusual and may provide enhanced sensing capabilities. Models for analyzing these responses are the subject of ongoing investigations.

4. Conclusions

In conclusion, we have demonstrated the potential of soft imprinting technology for fabricating plasmonic crystal sensors. Sensitivity maps of representative device were constructed from angle-dependent transmission experiments. The sensors exhibit high sensitivity when operated at certain angles. These angles correspond to locations in the plasmonic Brillouin zone where dispersion curves of unperturbed SPP modes converge. This observation may be important for future classes of plasmonic crystal biosensors.

Acknowledgments

We acknowledge the support of the U.S. Department of Energy (DEFG02-91-ER45439). All measurements reported here were carried out in the Laser and Spectroscopy Facility of the Frederick Seitz Materials Research Laboratory, University of Illinois, which is partially supported by the U.S. Department of Energy under grant DEFG02-91-ER45439.

#7370 - $15.00 US
Received 5 May 2005; revised 8 July 2005; accepted 10 July 2005
(C) 2005 OSA